Dalton Transactions

COMMUNICATION

View Article Online
View Journal | View Issue

Cite this: *Dalton Trans.*, 2015, **44**, 3536

Received 29th August 2014,
Accepted 8th October 2014

DOI: 10.1039/c4dt02649g

www.rsc.org/dalton

Convenient detection of metal–DNA, metal–RNA, and metal–protein adducts with a click-modified Pt(II) complex†

Alan D. Moghaddam,‡[a] Jonathan D. White,‡[a] Rachael M. Cunningham,[a,b] Andrea N. Loes,[a,b] Michael M. Haley[a] and Victoria J. DeRose*[a,b]

***cis*-[Pt(2-azido-1,3-propanediamine)Cl_2] is a reagent for high-yield post-treatment fluorescent labelling of Pt(II) biomolecular targets using click chemistry and exhibits a bias in conformational isomers in the context of duplex DNA. Pt–protein adducts are detected using BSA as a model. Following *in vivo* treatment, long-lived Pt–RNA adducts are detected on ribosomal RNA.**

Platinum(II)-based drugs are administered in many anticancer treatment regimes;[1] however, a broad identification of Pt-specific cellular targets is still lacking.[2] As Pt(II) compounds are effective nucleic acid crosslinking agents, they also have potential as structure probes in complex RNAs.[3] Click-functionalized Pt reagents provide a reactive handle for post-treatment labelling that would enable broad detection, isolation and identification of Pt-bound species. We recently described a new pyridine-based Pt click reagent, picazoplatin (**1**, Fig. 1).[4] Despite the wide use of click chemistry and importance of platinum therapeutics, only one other recently reported compound, an extended Pt-acridine therapeutic, is available for post-treatment click analysis.[5] In the case of picazoplatin, relatively slow reaction kinetics are built into the design of the parent compound picoplatin wherein the ring methyl shields Pt from substitution reactions.[6] Moreover, although in-cell use was demonstrated, analysis of cellular targets may be complicated by the potential for *trans*-labilization of the azide-functionalized picoline ring. New click-functionalized Pt(II) reagents are of great interest in order to take advantage of bioorthogonal approaches[7] for high-throughput identification of Pt-bound species *in vivo*.

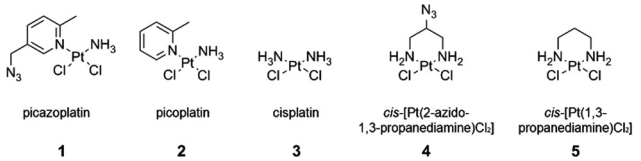

Fig. 1 Click-functionalized picazoplatin **1** and its parent picoplatin **2**, with cisplatin **3** and the 1,3-propanediamine derivatives **4** and **5**.

To provide a convenient and fast-reacting Pt(II)-azide click reagent, we have explored *cis*-[Pt(2-azido-1,3-propanediamine)-Cl_2] (**4**) in nucleic acid binding, protein binding, and click chemistry. While **4** has been previously used to create libraries of diazenecarboxamide–carboplatin conjugates,[8] to our knowledge it has not been applied as an agent for post-treatment labelling by click modification. Herein, we demonstrate efficient click reactivity of the DNA-bound compound and an unusual isomeric differentiation of **4** when bound to duplex DNA. Click fluorescent labelling of Pt-bound proteins is demonstrated in bovine serum albumin (BSA). The utility of this compound for *in vivo* studies is demonstrated by tracking Pt-bound ribosomes from cells treated with **4**.

DNA binding studies of **4** on a 13-nucleotide DNA containing a single GG site were analysed by dPAGE (Fig. 2). A higher yield of **4**-bound DNA is observed in comparison with the sterically-hindered **1**. Subsequent click reactivity with a dansyl alkyne fluorophore is seen in both cases.

To further quantify Pt binding and click reactivity of **4**, HPLC analysis was used with a short DNA hairpin sequence (TATGGTATTTTTATACCATA, HP). Upon Pt binding to the single GG site, two product peaks emerge that are distinct from the parent DNA peak. Both new peaks were confirmed by dPAGE to contain hairpin DNA bound by Pt (see ESI†). Both products contain one bound Pt(2-azido-1,3-propanediamine) as confirmed by identical 3+ charged ions in ESI-MS analysis (Fig. 3C). When reacted with dansyl alkyne, material in both product peaks yields clicked products as resolved by HPLC and identified by the fluorophore absorbance at 340 nm (>80% yield, see ESI†). Thus, this bimodal product distribution is hypothesized to originate from two different structural isomers of **4** bound to the asymmetric DNA strand. This

[a]*Department of Chemistry & Biochemistry, University of Oregon, Eugene, OR 97403-1253, USA*
[b]*Institute of Molecular Biology, University of Oregon, Eugene, OR 97403-1253, USA. E-mail: derose@uoregon.edu; Tel: +1-541-346-3568*

†Electronic supplementary information (ESI) available: Experimental procedures, additional HPLC and dPAGE characterization, ^{1}H, ^{13}C, and ^{195}Pt NMR spectra of **5**. See DOI: 10.1039/c4dt02649g

‡These authors contributed equally to this work.

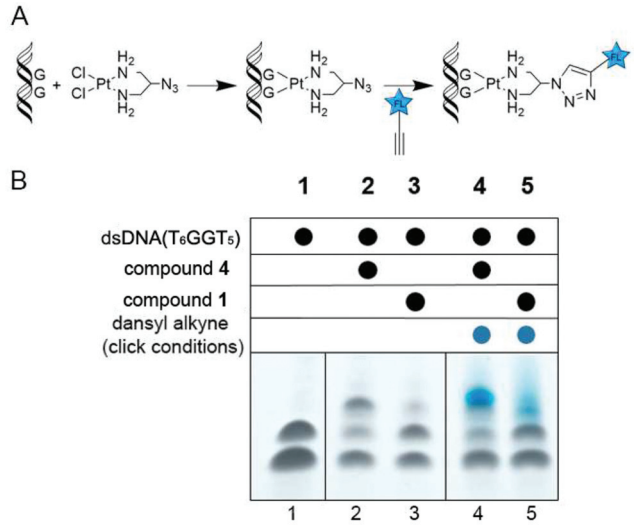

Fig. 2 (A) Reaction scheme for Pt binding and subsequent click to an alkyne fluorophore. (B) dPAGE analysis of dsDNA bound by picazoplatin (**1**) and *cis*-[Pt(2-azido-1,3-propanediamine)Cl_2] (**4**) and subsequently clicked to a dansyl alkyne fluorophore. The denatured DNA strands are visible in lane 1, while higher molecular weight Pt-bound species are visible in lanes 2 and 3. Click reaction results in fluorescence of the Pt–DNA band under UV light in lanes 4 and 5 (see ESI†).

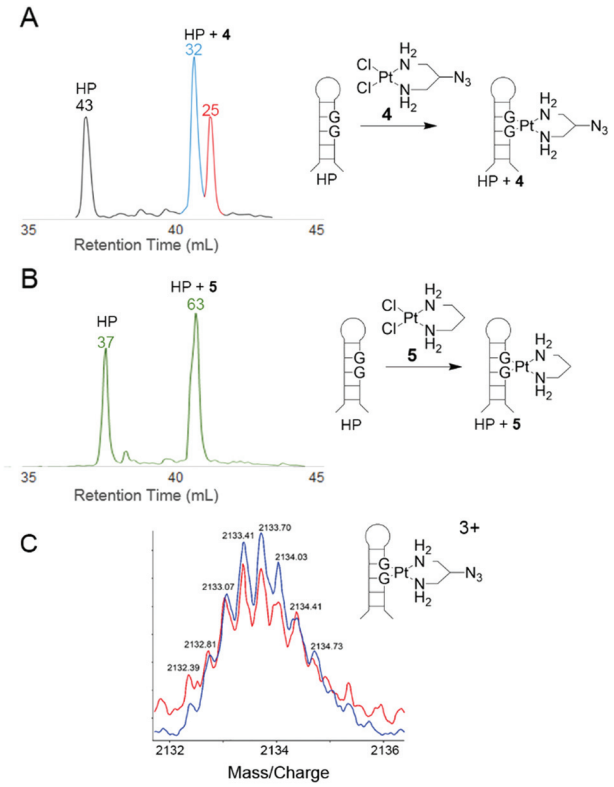

Fig. 3 HPLC absorbance traces at 260 nm for a short hairpin DNA sequence bound to (A) **4** and (B) **5**. Peaks observed at ~37 mL eluent volume are identified as unbound DNA, and peaks between ~40 and ~42 mL are Pt-bound DNA (55–65% yield). When **4** is bound to DNA, two peaks are resolved indicating the presence of non-equivalent Pt-bound species. Both collected fractions (blue and red traces) were analysed *via* ESI-MS, revealing that they contain the same 3+ charged species of **4**-bound DNA (C). Reaction with azide-free **5** yields a single product band (B, 55–65% yield). Normalized areas are indicated above peaks of interest.

hypothesis was tested with the analogous azide-free complex **5** (see ESI†).[9] As expected, the HPLC trace of DNA-bound **5** exhibits only one product peak (Fig. 3B), indicating that the 2-azido group of **4** creates structural isomers.

The two isomer products of **4**-treated hairpin DNA consistently yield non-equivalent peak areas, indicating preference of one conformation that is likely being dictated by the orientation of the azide relative to the helix. Supporting this, treatment of single-stranded DNA shows equivalent populations of both isomers (Fig. 4C), whereas the same sequence in duplex returns to an unequal population (Fig. 4D, see also ESI†).

Possible conformations of DNA-bound **4** are visualized (Fig. 4) in molecular models built by substituting **4** into the crystal structure of cisplatin-bound 12-mer DNA duplex (pdb: 3LPV).[10] Bond lengths and angles around the Pt(II) centre were fixed and the position of the DNA was locked (see ESI†), and equilibrium geometries of the two structural isomers were determined using molecular mechanics (MMFF). The resulting models show distinct geometric properties, with the azide oriented either toward the major groove or towards the phosphate backbone. In the denatured strands analysed by HPLC, these isomers must give rise to slight differences in hydrophobicity; resolution of such minor differences in oligonucleotides has precedent.[11,12] The inequivalent populations of isomers suggest that the helical structure of DNA has a direct impact on the preferred orientation of the azide substituent due to steric and electronic effects. Like the hairpin DNA, upon reaction with the dansyl alkyne fluorophore, **4**-bound T_6GGT_5 is converted into clicked products with yields that range from 80–90% (see ESI†).

In furthering the analysis of potential targets for Pt(II) compounds, bovine serum albumin (BSA) was also investigated as a model compound for the ability of **4** to bind and participate in post-treatment labelling of proteins. Previous studies have shown Pt-binding to Cys 34[13] following treatment of BSA with cisplatin. Here BSA is incubated with increasing equivalents of **4** followed by click to an alkyne-containing dansyl fluorophore (Fig. 5). Labelled protein was visualized by Coomassie staining and fluorescence imaging. Fluorescence is seen only in the **4**-treated samples and increases in a dose-dependent manner (Fig. 5, lanes 2–4). Fluorescence is also only observed in reactions containing both **4** and the Cu catalyst.

Ultimately, the power of clickable Pt compounds is to identify and analyze *in vivo* targets. In contrast to cisplatin, Pt(II) compounds with small chelating amine ligands such as ethylenediamine and 1,3-propanediamine are better tolerated by cells, making them particularly attractive as potential *in vivo* crosslinking reagents.[14] We have previously shown significant accumulation of Pt on cellular RNA following treatment with cisplatin, with major accumulation being on ribosomal

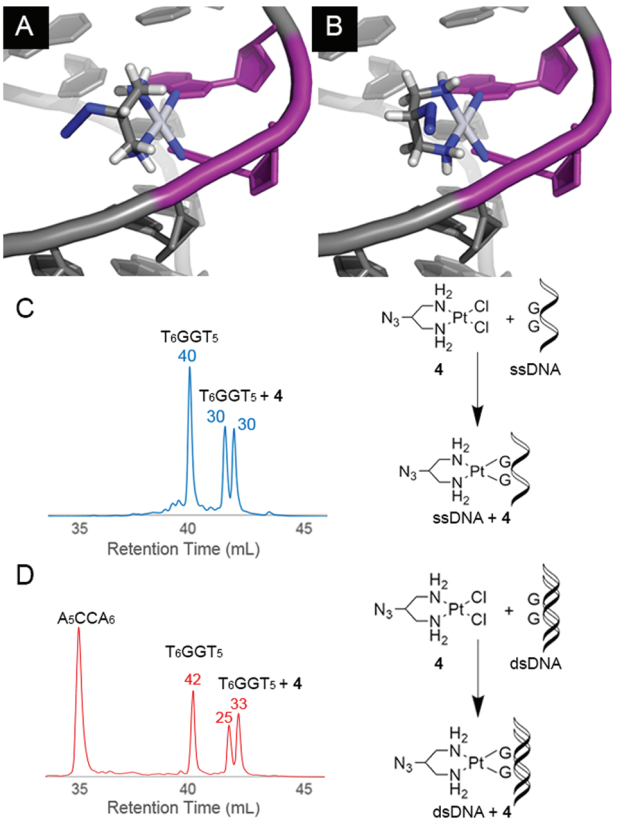

Fig. 4 Molecular modelling (MMFF) of the two possible isomers of **4**-bound double-stranded DNA with the azide oriented in towards (A) or out from (B) the centre of the helix. In the helical conformation of A as shown, the azide moiety is less solvent exposed than in B. Models were generated by substituting **4** into the crystal structure of cisplatin-bound DNA (PDB: 3LPV, see ESI†). The adjacent Pt-bound guanines of the intrastrand crosslink are shaded purple. HPLC absorbance traces at 260 nm for **4** reacted with (T_6GGT_5) as a single-strand (C, 55–65% yield) or in duplex (D, 55–65% yield). Normalized areas are indicated above peaks of interest. When reacted with the single-strand sequence, isomers of **4**-bound DNA show equal population (ratio = 0.96 ± 0.05; see ESI† for data in triplicate) whereas they are unequal for the duplex (ratio = 1.3 ± 0.09; see also ESI†).

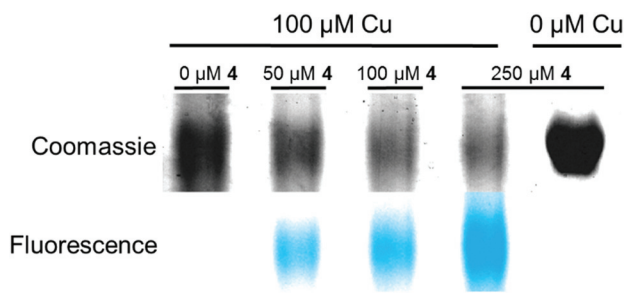

Fig. 5 Fluorescent labelling by click chemistry of **4**-treated bovine serum albumin (BSA) with a dansyl alkyne fluorophore. Lanes 2–4 contain BSA incubated in the presence of $CuSO_4$ post Pt treatment and show a dose-dependent increase in fluorescent signal with respect to the concentration of **4**. Lanes 1 and 5 shows that fluorescent labelling is also dependent on the presence of both **4** and the Cu catalyst.

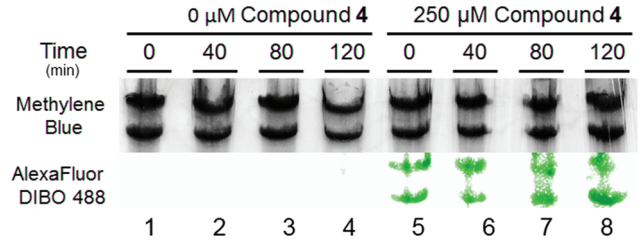

Fig. 6 Fluorescent labelling by click chemistry of rRNA extracted from **4**-treated *S. cerevisiae*. 25S and 18S rRNA extracted from *S. cerevisiae* treated with 0 μM or 250 μM **4** for 6 h and resuspended in drug-free media for 0–120 min. All samples were subsequently treated with 250 μM Alexa Fluor 488 DIBO (16 h, 37 °C).

RNA.[15,16] Here, we tracked the lifetime of Pt–RNA adducts using **4**, and find surprising longevity of Pt adducts on ribosomal RNA. *S. cerevisiae* was treated with 0 μM and 250 μM **4** for 6 h and then re-suspended in fresh media. Cells resuspended in drug-free media showed growth similar to untreated control cells, consistent with the relatively low toxicity of **4** and in contrast to treatment with cisplatin.[15] To determine whether Pt–rRNA adducts were quickly degraded or long-lived, RNA was extracted from cells at various timepoints and accumulated Pt detected following click labelling with Alexa Fluor 488 DIBO (Fig. 6). Lanes 1–4 contain rRNA isolated from untreated cells subjected to the same click labelling protocol. The absence of fluorescence in these lanes indicates the absence of nonspecific labelling during the DIBO/click procedure. Lanes 5–8 contain rRNA isolated from treated cells after up to 2 h in **4**-free media. The normalized fluorescence per rRNA band shows no significant loss in Pt–RNA adducts, meaning that platinated ribosomes persist in doubling cells and that the majority of them are not targeted for fast degradation. The persistence of the fluorescent labelling even after 120 min post-treatment demonstrates the efficacy of **4** in post-labelling strategies to ascertain possible Pt(II) cellular targets.

Conclusions

This work demonstrates the ability of azide-modified Pt(II) compound **4** to readily bind oligonucleotides and proteins and subsequently undergo click reactions for post-treatment fluorescent labelling. This demonstrated reactivity of **4** expands the array of available azide-modified Pt(II) reagents to be used in post-treatment target analysis. In comparison with recently reported **1**, **4** exhibits greatly increased efficiency in target binding. HPLC analysis and molecular modelling suggest formation of two different isomers of **4**-bound DNA adducts, hypothesized to be biased by the orientation of the azide moiety of **4** in relation to the helical structure of DNA. Efforts to discern differences in click reactivity between the two isomers are currently underway in our laboratory, as well as efforts utilizing clickable Pt(II) reagents as RNA crosslinking agents to quantify and isolate platinum-bound species *in cellulo*.

Acknowledgements

We thank the National Science Foundation (CHE-1153147) for support of this research.

Notes and references

1 (*a*) B. W. Harper, A. M. Krause-Heuer, M. P. Grant, M. Manohar, K. B. Garbutcheon-Singh and J. R. Aldrich-Wright, *Chem. – Eur. J.*, 2010, **16**, 7064–7077; (*b*) P. J. Dyson and G. Sava, *Dalton Trans.*, 2006, 1929–1933; (*c*) D. Wang and S. J. Lippard, *Nat. Rev. Drug Discovery*, 2005, **4**, 307–320.

2 (*a*) G. Sava, G. Jaouen, E. A. Hillard and A. Bergamo, *Dalton Trans.*, 2012, **41**, 8226–8234; (*b*) A. Casini and J. Reedijk, *Chem. Sci.*, 2012, **3**, 3135–3144; (*c*) E. R. Guggenheim, D. Xu, C. X. Zhang, P. V. Chang and S. J. Lippard, *ChemBioChem*, 2009, **10**, 141–157; (*d*) E. Wexselblatt, E. Yavin and D. Gibson, *Inorg. Chim. Acta*, 2012, **393**, 75–83.

3 (*a*) E. G. Chapman and V. J. DeRose, *J. Am. Chem. Soc.*, 2012, **134**, 256–262; (*b*) E. G. Chapman and V. J. DeRose, *J. Am. Chem. Soc.*, 2010, **132**, 1946–1952; (*c*) A. A. Hostetter, E. G. Chapman and V. J. DeRose, *J. Am. Chem. Soc.*, 2009, **131**, 9250–9257.

4 J. D. White, M. F. Osborn, A. D. Moghaddam, L. E. Guzman, M. M. Haley and V. J. DeRose, *J. Am. Chem. Soc.*, 2013, **135**, 11680–11683.

5 (*a*) S. Ding, X. Qiao, J. Suryadi, G. S. Marrs, G. L. Kucera and U. Bierbach, *Angew. Chem. Int. Ed.*, 2013, **52**, 3350–3354; (*b*) X. Qiao, S. Ding, F. Liu, G. L. Kucera and U. Bierbach, *J. Biol. Inorg. Chem.*, 2014, **19**, 415–426.

6 (*a*) L. Kelland, *Nat. Rev. Cancer*, 2007, **7**, 573–584; (*b*) F. I. Raynaud, F. E. Boxall, P. M. Goddard, M. Valenti, M. Jones, B. A. Murrer, M. Abrams and L. R. Kelland, *Clin. Cancer Res.*, 1997, **3**, 2063–2074; (*c*) Y. Chen, Z. Guo, S. Parsons and P. J. Sadler, *Chem. – Eur. J.*, 1998, **4**, 672–676; (*d*) Y. Chen, Y. Z. Guo, J. A. Parkinson and P. J. Sadler, *Dalton Trans.*, 1998, 3577–3586; (*e*) L. R. Kelland, S. Y. Sharp, C. F. O'Neill, F. I. Raynaud, P. J. Beale and I. R. Judson, *J. Inorg. Biochem.*, 1999, **77**, 111–115.

7 (*a*) J. C. Jewett and C. R. Bertozzi, *Chem. Soc. Rev.*, 2010, **39**, 1272–1279; (*b*) H. C. Kolb, M. G. Finn and K. B. Sharpless, *Angew. Chem. Int. Ed.*, 2001, **40**, 2004–2021.

8 (*a*) N. Stojanovic, D. Urankar, A. Brozovic, A. Ambriović-Ritsov, M. Osmak and J. Košmrlj, *Acta Chim. Slov.*, 2013, **60**, 368–374; (*b*) D. Urankar and J. Košmrlj, *Inorg. Chim. Acta*, 2010, **363**, 3817–3822.

9 J. Zhang, L. Ma, H. Lu, Y. Wang, S. Li, S. Wang and G. Zhou, *Eur. J. Med. Chem.*, 2012, **58**, 281–286.

10 R. C. Todd and S. J. Lippard, *J. Inorg. Biochem.*, 2010, **104**, 902–908.

11 (*a*) W. L. Ward and V. J. DeRose, *RNA*, 2012, **18**, 16–23; (*b*) J. K. Frederiksen and J. A. Piccirilli, *Methods in Enzymology*, ed. D. Herschlag, Academic Press, 2009, ch. 14, vol. 468, pp. 289–309.

12 M. J. Bloemink, R. J. Heetebrij, K. Inagaki, Y. Kidani and J. Reedijk, *Inorg. Chem.*, 1992, **31**, 4656–4661.

13 A. Sugii, K. Nishimura, K. Harada, M. Nakayama and S. Masuda, *Chem. Pharm. Bull.*, 1991, **39**, 408–410.

14 N. H. Kuroda, Y. Hayami, O. K. Ekimoto and H. K. Takahashi, *Chem. Pharm. Bull.*, 1989, **37**, 2406–2409.

15 A. A. Hostetter, M. F. Osborn and V. J. DeRose, *ACS Chem. Biol.*, 2012, **7**, 218–225.

16 M. F. Osborn, J. D. White, M. M. Haley and V. J. DeRose, *ACS Chem. Biol.*, 2014, **9**, 2404–2411.